

Joint MAP Equalization and Channel Estimation for Frequency-Selective and Frequency-Flat Fast-Fading Channels

Linda M. Davis, *Member, IEEE*, Iain B. Collings, *Member, IEEE*, and Peter Hoeher, *Senior Member, IEEE*

Abstract—This paper presents a new fractionally-spaced maximum *a posteriori* (MAP) equalizer for data transmission over frequency-selective fading channels. The technique is applicable to any standard modulation technique. The MAP equalizer uses an expanded hypothesis trellis for the purpose of joint channel estimation and equalization. The fading channel is estimated by coupling minimum mean square error techniques with the (fixed size) expanded trellis. The new MAP equalizer is also presented in an iterative (turbo) receiver structure. Both uncoded and conventionally coded systems (including iterative processing) are studied. Even on frequency-flat fading channels, the proposed receiver outperforms conventional techniques. Simulations demonstrate the performance of the proposed equalizer.

Index Terms—Communication systems, fading channels, MAP estimation, equalization.

I. INTRODUCTION

MOBILE radio communication channels are time-varying channels. They are characterized by the presence of both delay and Doppler spreading. Depending on the delay spread and the data rate, the channel may be approximately flat fading (e.g., rural areas, narrowband systems), or frequency-selective (e.g., hilly terrain, wideband systems). Frequency-selective channels produce intersymbol interference (ISI). The ISI can be modeled with several filter taps which represent attenuation along each of the delay paths causing the ISI [1], [2]. A channel may also be fast or slow fading, depending on the Doppler spread of the channel and the data rate. Slow fading can easily be tracked by the receiver, whereas fast fading requires more sophisticated channel estimation. With the recent allocation of higher frequency bands for mobile communications comes the reality of channels that simultaneously exhibit fast-fading and ISI.

This paper focuses on fast-fading frequency-selective channels, although frequency-flat fast-fading channels are also con-

sidered to be a specific case. Importantly, we consider the general equalization problem for any of the standard modulation schemes.

The standard approach to equalization with unknown channels is to generate a single channel estimate based on the statistics of the channel [3]. This requires either a training sequence or a delayed decision-directed approach. However, a more integrated technique, such as maximum likelihood sequence estimation (MLSE) linked with per-survivor processing (PSP), provides superior performance [4]. More recently, the advent of “turbo processing” [5], has revitalized interest in maximum *a posteriori* (MAP) equalization in preference to MLSE [6], [7].

The MAP algorithm is a symbol-by-symbol estimator which accepts observations (in the form of matched filter outputs) together with *a priori* symbol probabilities (soft inputs) and produces *a posteriori* symbol probabilities. The decoded symbol is declared to be that with the maximum *a posteriori* probability. Thus, the MAP algorithm minimizes the bit error rate (BER). When the probabilities are retained as soft outputs, the MAP equalizer is suited to receiver structures in which subsequent stages (e.g., outer decoding) utilize soft decisions. In this paper, we consider the block-processing MAP equalizer [8], which may be implemented using forward-backward recursions [9]. Online (forward only) versions of the MAP algorithm for equalization and decoding are also possible [10]–[13]. These algorithms may be directly applied in fading systems where perfect channel state information is assumed to be available at the receiver.

This paper presents an extension to the block-processing MAP equalizer for the case where the channel is not assumed to be known. As with standard Viterbi algorithms, the operation of the MAP equalizer may be represented using a state trellis [1]. In this paper, we use an expanded trellis so as to include extra memory for measuring the channel. This allows joint channel estimation and equalization. Expansion of the state space is made possible by the fact that the low-pass nature of the fading effectively introduces correlation into the received signal. The expanded state can then be used to form separate channel estimates for each trellis state. Conceptually, this is similar to PSP. However, per-survivor techniques are only applicable to MLSE equalizers. MAP equalizers require channel estimates based on the trellis state since there is no concept of a surviving sequence.

For our new equalizer, the size of the expanded state space is fixed, and minimum mean square error (MMSE) techniques are proposed for forming channel estimates. This follows the

Paper approved for publication by M. Z. Win, the Editor for Equalization and Diversity of the IEEE Communications Society. Manuscript received December 27, 1998; revised December 28, 1999, September 20, 2000, and May 24, 2001. This paper was presented in part at the IEEE Globecom'98 CTMC, Sydney, Australia, November 1998.

L. M. Davis is with Bell Laboratories, Lucent Technologies, Lucent Centre, North Ryde, NSW 2113, Australia (e-mail: lindadavis@lucent.com).

I. B. Collings is with the School of Electrical and Information Engineering, University of Sydney, Sydney, NSW 2006, Australia (e-mail: iain@ee.usyd.edu.au).

P. Hoeher is with the Information & Coding Theory Laboratory, Faculty of Engineering, University of Kiel, D-24143 Kiel, Germany (e-mail: ph@techfak.uni-kiel.de).

Publisher Item Identifier S 0090-6778(01)10623-9.

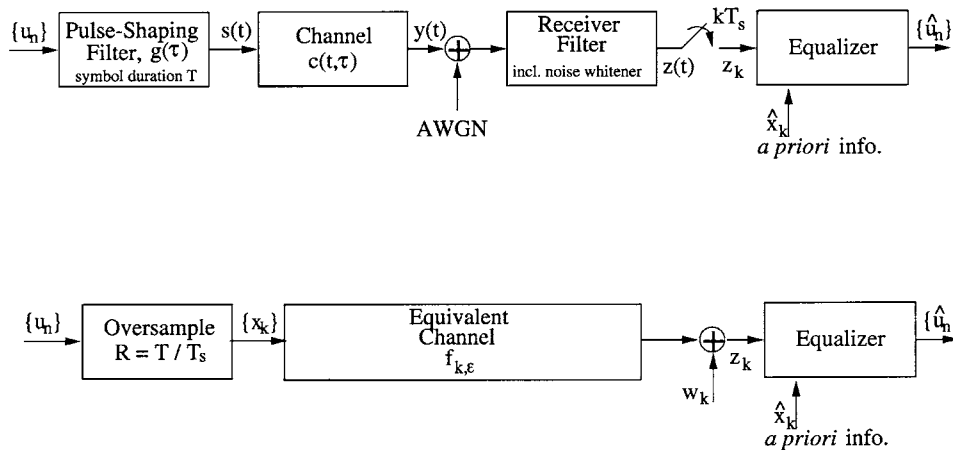


Fig. 1. Baseband transmission system model.

predictive receiver approach of [14], however, in that case the expansion was limited to continuous phase-modulated (CPM) or phase-shift-keyed (PSK) transmission. It is also in contrast to the Bayesian MAP (forward only) equalizers proposed in [15], [16] where the state space grows exponentially with time unless pruning or decision feedback techniques are applied (see [17] and [18] and references therein).

Our new fractionally-spaced equalizer is suitable for both equalization of frequency-selective channels (i.e., exhibiting ISI) and demodulation of frequency-flat fast-fading channels and is related to the contributions of [4], [8], [19], [20], and [14]. Our equalizer is applicable to transmission systems with arbitrary modulation schemes and arbitrary pulse shaping. In particular, the algorithm is not restricted to constant amplitude signals. We show that the predictive demodulator of [14], which is restricted to CPM or PSK transmission over flat fading channels, is a special case.

Simulations are used to demonstrate the performance of our new equalizer in an uncoded phase-shift keyed (PSK) system. The importance of the MAP equalizer lies in its application to turbo processing. The structure of the turbo processing receiver is reviewed and the performance of the turbo receiver for frequency-selective channels is demonstrated by simulation.

II. TRANSMISSION SYSTEM MODEL

The transmission of data symbols over either a frequency-selective or frequency-flat fading channel is shown in Fig. 1. In this paper, we adopt the equivalent discrete model [2], [1], [21] with oversampling.

The data sequence (of length N) is designated $\{u_n\}$. It is transmitted over the channel using Q -ary symbols of period T , with band-limited pulse shape $g(\tau)$. The physical frequency-selective fading channel has impulse response $c(t, \tau)$. The physical channel is usually assumed to have Gaussian fading statistics, thus resulting in a Rayleigh or Rician channel. When assuming the wide-sense-stationary and uncorrelated scatterers (WSSUS) model, the scattering function (or delay-Doppler power spectrum) completely describes the channel statistics. Additive white Gaussian noise (AWGN) is introduced at the receiver input, where the received signal

is filtered and sampled at a rate of $1/T_s$, so that the discrete received signal z_k is oversampled at the rate $R = T_s/T \leq 1$.

The discrete equivalent channel $f_{k,\epsilon}$ describes the pulse-shaping filter, the physical channel, the receiver filter, and the sampling [1]. Thus, the taps are generally correlated even if the scatterers in the physical channel are uncorrelated [22]. The samples, z_k , are a sufficient set of statistics for the receiver, and the discrete equivalent finite impulse response (FIR) transmission model is given by

$$z_k = \sum_{\epsilon=0}^{\ell-1} x_{k-\epsilon} f_{k,\epsilon} + w_k \quad k = 0 \dots N/R - 1 \quad (1)$$

where the sequence $\{x_k\}$ is an oversampled version of $\{u_n\}$

$$x_k = \begin{cases} u_n, & \text{for } n = kR \text{ integer} \\ 0, & \text{otherwise} \end{cases} \quad (2)$$

The complex-valued noise samples, w_k , are generally colored by virtue of the anti-aliasing filter at the receiver input. Note that we use k to index quantities sampled at the higher rate $1/T_s = 1/RT$ and n to index quantities at the symbol rate $1/T$.

It is apparent from (1) that each sample, z_k , at the sample rate, $1/T_s$, depends on $\{x_{k-\ell+1} \dots x_k\}$ (i.e., $\ell - 1$ values previous to x_k interfere with the output z_k). Therefore, there are $L - 1 = \lceil (\ell - 1)R \rceil$ additional bits of ISI at the symbol rate. Thus, for Q -ary transmission, the trellis for MLSE has Q^{L-1} states ($L > 1$).

III. MAP EQUALIZATION

Here we review the MAP algorithm for symbol-by-symbol detection of the transmitted sequence $\{u_n\}$. In this section, we assume that *perfect channel state information*, $f_{k,\epsilon}$, is available at the receiver. In Section IV, our new method for obtaining channel estimates based on expanding the trellis will be presented.

The MAP algorithm calculates the *a posteriori* probability of each transmitted symbol, i.e., $\Pr(u_n = q | Z_0^{N/R-1}, \theta)$, for each of the Q -ary symbols, q , where $Z_0^{k_2}$ is the set of observations $\{z_{k_1} \dots z_{k_2}\}$ and θ represents the channel model. The decoded symbol is declared to be that with the maximum *a posteriori*

probability. When soft outputs are required (e.g., in turbo processing), the *a posteriori* probabilities (APP) are retained, and the algorithm may be referred to as the APP algorithm.

For $R = 1$, we obtain a symbol-spaced MAP equalizer; for $R < 1$, we obtain a fractionally-spaced equalizer. In both cases, the operation of the MAP algorithm may be represented using a symbol-spaced state trellis.

The j th state of the trellis at time n is labeled $S_{n,j}$. This state represents one of the Q^{L-1} possible values for $\{u_{n-L+2} \dots u_n\}$. We denote the particular value by $\{\tilde{u}_{n-L+2,j} \dots \tilde{u}_{n,j}\}$, where tilde indicates a hypothesized value. Of course, for ISI channels and for our expanded trellis (see Section IV), more than one $S_{n,j}$ will correspond to a particular $u_n = q$. Thus,

$$\Pr(u_n = q \mid Z_0^{N/R-1}, \theta) = \sum_{j: \tilde{u}_n = q} \Pr(S_{n,j} \mid Z_0^{N/R-1}, \theta) \quad (3)$$

The *a posteriori* state probabilities, $\gamma_{n,j} = \Pr(S_{n,j} \mid Z_0^{N/R-1}, \theta)$, can be calculated using the forward-backward procedure [9]. The forward variable is $\alpha_{n,j} = \Pr(S_{n,j}, Z_0^{(n+1)/R-1} \mid \theta)$. The backward variable is $\beta_{n,j} = \Pr(Z_{(n+1)/R}^{N/R} \mid S_{n,j}, \theta)$. Denoting the *a priori* transition probability from state $S_{n-1,i}$ to state $S_{n,j}$ by $a_{n,ij}$, and the probability of observations $Z_{n/R}^{(n+1)/R-1}$ on that transition by $b_{n,ij}$, the recursions for the forward and backward variables are

$$\alpha_{n,j} = \sum_{i=1}^{Q^*} b_{n,ij} a_{n,ij} \alpha_{n-1,i} \quad (4)$$

$$\beta_{n,i} = \sum_{j=1}^{Q^*} b_{n+1,ij} a_{n+1,ij} \beta_{n+1,j} \quad (5)$$

where Q^* is the number of states in the trellis. The initial values $\alpha_{-1,j}$ may be chosen to be equal (i.e., $1/Q^*$), or alternatively (without affecting any result) $\alpha_{-1,1} = 1$ and $\alpha_{-1,j} = 0$ for $j = 2, \dots, Q^*$. At the end of the block, $\beta_{N,j} = 1/Q^*$ for $j = 1, \dots, Q^*$ should be chosen, unless zero-tailing is used to ensure that $\beta_{N,1} = 1$ and $\beta_{N,j} = 0$ for $j = 2, \dots, Q^*$. It has been shown that the impact of zero-tailing on performance is not significant, especially for a large block size N .

The *a posteriori* state probabilities are then given by

$$\gamma_{n,j} = \frac{\alpha_{n,j} \beta_{n,j}}{\sum_{i=1}^{Q^*} \alpha_{n,i} \beta_{n,i}} \quad (6)$$

The *a priori* state transition probabilities are derived from the *a priori* information provided to the equalizer (soft inputs)

$$\begin{aligned} a_{n,ij} &= \Pr(S_{n,j} \mid S_{n-1,i}, \theta) \\ &= \Pr(\tilde{u}_{n-L+2,j} \dots \tilde{u}_{n,j} \mid \tilde{u}_{n-L+1,i} \dots \tilde{u}_{n-1,i}, \theta). \end{aligned} \quad (7)$$

MAP and MLSE algorithms are usually based on the assumption of AWGN, w_k , to simplify calculation of the observation probabilities. This approach is adopted here, where the variance is $\sigma_w^2 \triangleq (1/2)E[w_k w_k^*] = N_o/(2T_s)$. $N_o/2$ is the two-sided

spectral noise density [1]. The observation probabilities $b_{n,ij}$ are then given by

$$\begin{aligned} b_{n,ij} &= \Pr\left(Z_{n/R}^{(n+1)/R-1} \mid S_{n-1,i}, S_{n,j}, \theta\right) \\ &= \prod_{k=n/R}^{(n+1)/R-1} \frac{1}{\sqrt{2\pi\sigma_w^2}} e^{-\frac{1}{2\sigma_w^2} |z_k - \hat{z}_{k,ij}|^2} \end{aligned} \quad (8)$$

where

$$\hat{z}_{k,ij} = \sum_{\epsilon=0}^{\ell-1} \tilde{x}_{k-\epsilon,ij} f_{k,\epsilon}. \quad (9)$$

For computational savings, the MAP equalizer may be implemented in the log domain without loss of optimality [12], [13].

The next section describes how the channel response $f_{k,\epsilon}$ is jointly estimated with the data sequence. In fact, there will be a different channel estimate for each transition. Under the assumption of a transition from state i to state j , the channel estimate is denoted $\hat{f}_{k,\epsilon,ij}$. When the channel is being estimated, the variance σ_w^2 , in (8), will be replaced by $\hat{\sigma}_{k,ij}^2$ which accounts for the noise and the extra variance due to channel estimation errors.

Pilot symbols can be used to resolve phase ambiguity. The formulation of the MAP equalizer is such that we do not need to distinguish between a pilot symbol and an unknown data symbol in the MAP algorithm. Whenever there is a pilot symbol, the *a priori* transition probabilities (contained in the input information) corresponding to that symbol are set to one. The MAP algorithm handles this *a priori* information in exactly the same way as *a priori* information on transitions corresponding to an unknown data symbol. For the pilot symbol, it transpires that some transitions (and therefore states) in the trellis have zero probability. Hence, phase ambiguity is resolved. In Section V-A, we will investigate the use of pilot symbols further.

When the *a posteriori* probabilities are retained, the symbol-by-symbol APP algorithm is a soft-input soft-output technique, and thus the new equalizer may be applied in an iterative (turbo) processing receiver. The turbo receiver structure consists of an APP equalizer and an APP decoder separated by a deinterleaver and interleaver, as shown in Fig. 2.

IV. MMSE CHANNEL ESTIMATION

In the previous section, we reviewed the MAP algorithm for symbol-by-symbol equalization where channel estimates were available at the receiver. Now we consider how those estimates can be obtained using MMSE estimation techniques.

A. General Case: Frequency-Selective Channels

Consider first the per-survivor MLSE equalizer [4]. The transition metric $b_{n,ij}$ (8) from trellis state $S_{n-1,i}$ to state $S_{n,j}$ is formed from $Z_{n/R}^{(n+1)/R-1}$ and the corresponding estimates $\hat{z}_{k,ij}$ given by (9), i.e., $\hat{Z}_{n/R}^{(n+1)/R-1}$. The true channel state information $f_{k,\epsilon}$ is replaced by an estimate $\hat{f}_{k,\epsilon,ij}$ obtained using the observations and the hypothesis along the path which has survived to state $S_{n-1,i}$ (e.g., this is done using a Kalman filter or

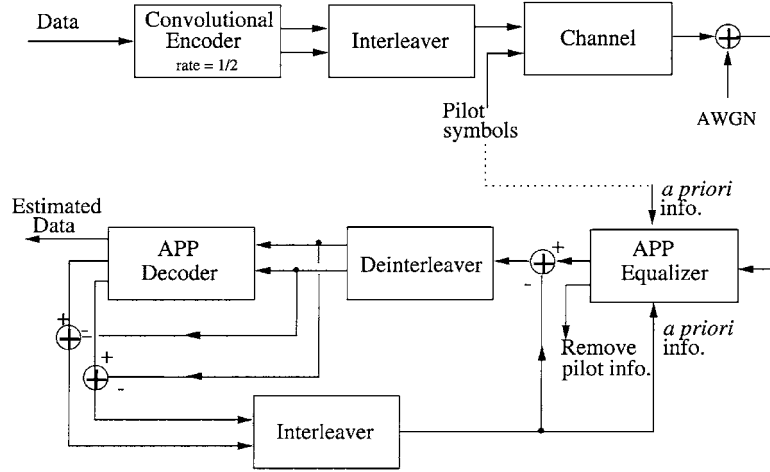


Fig. 2. Turbo receiver.

related algorithms with slightly reduced complexity [21], [20], [23]).

In contrast, with MAP equalization there is no concept of a surviving path to state $S_{n-1,i}$. Previously, work has been done to couple the MAP algorithm to a *single* channel estimator [24]. Instead, here we adopt a more sophisticated and general approach. It turns out that the work of [14] can be viewed as a special case.

In this paper, we *expand* the state space of the trellis to enable us to form channel estimates for each state. The states in the expanded trellis contain the extra information needed for the channel estimates in addition to the channel memory (i.e., ISI) information. When p additional samples of z_k and hypotheses \tilde{x}_k (at the sample rate) are used in the estimation, the expanded trellis has $Q^{\lceil(\ell+p-1)R\rceil}$ states. The expanded trellis state represents $\{\tilde{u}_{n-L-P+2,j} \dots \tilde{u}_{n,j}\}$ where $P = \lceil(\ell + p - 1)R\rceil - \lceil(\ell - 1)R\rceil$ additional symbols are included for the purposes of channel estimation.

So far, we have discussed forming estimates of the channel $\hat{f}_{k,\epsilon,ij}$ in order to calculate $\hat{z}_{k,ij}$ in (9) for the branch metrics for the MAP equalizer. However, in this section, we directly evaluate the MMSE estimates, $\hat{z}_{k,ij}$, without explicitly estimating $\hat{f}_{k,\epsilon,ij}$.

For our expanded trellis, the estimates $\hat{z}_{k,ij}$ (one for each state transition i to j), are calculated using the observations $\{z_k \dots z_{k-p}\}$ and the hypotheses $\{\tilde{x}_k \dots \tilde{x}_{k-p} \dots \tilde{x}_{k-\ell+1-p}\}$. This is achieved with a MMSE linear predictor. First, we write the observation equation [from (1)] in vector-matrix notation¹

$$\mathbf{z}_{k-1} = \mathbf{X}_{k-1} \mathbf{g}_{k-1} + \mathbf{w}_{k-1} \quad (10)$$

where $\mathbf{z}_{k-1} = [z_{k-p}, \dots, z_{k-1}]^T$, and $\mathbf{w}_{k-1} = [w_{k-p}, \dots, w_{k-1}]^T$, are $p \times 1$ vectors, and

$$\mathbf{X}_{k-1} = \begin{bmatrix} \mathbf{x}_{k-p}^T & \mathbf{0} & \dots & \mathbf{0} \\ \mathbf{0} & \ddots & & \vdots \\ \vdots & & \ddots & \mathbf{0} \\ \mathbf{0} & \dots & \mathbf{0} & \mathbf{x}_{k-1}^T \end{bmatrix}$$

¹Note: all vectors are defined as column vectors and designated with bold lower case; all matrices are given in bold upper case; $(\cdot)^T$ denotes transpose, $(\cdot)^*$ denotes complex conjugate and $(\cdot)^H$ denotes Hermitian (i.e., complex conjugate) transpose.

is a $p \times p\ell$ matrix, where $\mathbf{x}_k = [x_k \dots x_{k-\ell+1}]^T$. The $p\ell \times 1$ vector of channel coefficients $\mathbf{g}_{k-1} = [f_{k-p}^T, \dots, f_{k-1}^T]^T$, is made up of $\ell \times 1$ vectors $\mathbf{f}_k = [f_{k,0} \dots f_{k,\ell-1}]^T$. In this notation, $z_k = \mathbf{x}_k^T \mathbf{f}_k + w_k$. The estimate $\hat{z}_{k,ij}$ is obtained by prediction and is of the form

$$\hat{z}_{k,ij} = \mathbf{h}_{ij}^T \mathbf{z}_{k-1} \quad (11)$$

where, of course, the $p \times 1$ vector of channel coefficients \mathbf{h}_{ij} is possibly different for each transition in the trellis. Clearly there will be a different estimate, $\hat{z}_{k,ij}$, for each transition in the trellis.

We now need to calculate the vectors \mathbf{h}_{ij} . For what follows, we omit the subscripts $\{\cdot\}_{k,ij}$ and use only the tilde to indicate matrix values under the hypothesis of an ij transition. Minimizing the mean square error, $\sigma_{k,ij}^2 = E[(z_k - \hat{z}_{k,ij})^2 | \tilde{x}_{k,ij} \dots \tilde{x}_{k-p,ij} \dots \tilde{x}_{k-\ell+1-p,ij}]$, gives

$$\mathbf{h}_{k,ij}^T = \tilde{\mathbf{x}}^T \mathbf{R}_1 \tilde{\mathbf{X}}^H (\tilde{\mathbf{X}} \mathbf{R}_2 \tilde{\mathbf{X}}^H + N_o \mathbf{I})^{-1} \quad (12)$$

where the matrices relating to the channel covariance are $\mathbf{R}_1 = E[\mathbf{f}_k \mathbf{g}_{k-1}^H]$ which is $\ell \times p\ell$, and $\mathbf{R}_2 = E[\mathbf{g}_{k-1} \mathbf{g}_{k-1}^H]$ which is $p\ell \times p\ell$. Here, \mathbf{R}_1 and \mathbf{R}_2 are assumed to be known (from the scattering function of the channel and the transmitter pulse shape).

We can now calculate the branch metrics in the MAP equalizer by substituting the following expressions into (8):

$$\hat{z}_{k,ij} = \tilde{\mathbf{x}}^T \mathbf{R}_1 \tilde{\mathbf{X}}^H (\tilde{\mathbf{X}} \mathbf{R}_2 \tilde{\mathbf{X}}^H + N_o \mathbf{I})^{-1} \mathbf{z}_{k-1} \quad (13)$$

$$\hat{\sigma}_{k,ij}^2 = \sigma_z^2 - \tilde{\mathbf{x}}^T \mathbf{R}_1 \tilde{\mathbf{X}}^H (\tilde{\mathbf{X}} \mathbf{R}_2 \tilde{\mathbf{X}}^H + N_o \mathbf{I})^{-1} \tilde{\mathbf{X}} \mathbf{R}_1 \tilde{\mathbf{x}}^* \quad (14)$$

where $\sigma_z^2 = E[z_k z_k^* | \tilde{\mathbf{x}}_k] = \tilde{\mathbf{x}}^T E[\mathbf{f}_k \mathbf{f}_k^H] \tilde{\mathbf{x}}^* + \sigma_w^2$. Since the hypotheses, $\tilde{\mathbf{X}}$ and $\tilde{\mathbf{x}}$, depend only on the index of the preceding state, i , and the transition defined by ij , we note that the MMSE coefficients $\mathbf{h}_{k,ij}$ and the prediction error variance $\hat{\sigma}_{k,ij}^2$ are independent of k and can be precalculated.

Importantly with this approach, we are able use direct MMSE estimates $\hat{z}_{k,ij}$ for the outputs corresponding to each hypothesis. Note that this estimate is calculated independently for each time index k and there is no initialization required. Naturally, at the start of any processing block, it is not possible to use p samples

for prediction, since there are not that many available. The predictor coefficients can be recalculated for the number of samples available.

We note that it is also possible to use an MMSE filter to obtain the channel estimates (the channel estimate at time k is obtained from data and the hypothesis up to time k), as opposed to using a predictor (where the estimate at time k is obtained using data and the hypotheses up to time $k - 1$).

B. Special Case: Flat Fading Channels With CPM or PSK

In this section, we consider the special case of flat fading channels (i.e., $\ell = 1$), in particular in conjunction with constant amplitude transmitted symbols. Without loss of generality, the symbol magnitude can be considered to be unity. Thus, $\tilde{\mathbf{X}}\tilde{\mathbf{X}}^H = \mathbf{I}$, the $p \times p$ identity matrix. It follows then that

$$(\tilde{\mathbf{X}}\mathbf{R}_2\tilde{\mathbf{X}}^H + N_o\mathbf{I})^{-1} = \tilde{\mathbf{X}}(\mathbf{R}_2 + N_o\mathbf{I})^{-1}\tilde{\mathbf{X}}^H \quad (15)$$

by the matrix inversion lemma.

Note that, in the flat fading case, \mathbf{R}_1 becomes a $1 \times p$ row vector and thus

$$\hat{z}_{k,ij} = \tilde{x}_k \mathbf{R}_1 (\mathbf{R}_2 + N_o\mathbf{I})^{-1} \tilde{\mathbf{X}}^H \mathbf{z}_{k-1}. \quad (16)$$

We can now show that the demodulator of [14] for transmission of CPM, or alternatively PSK with one sample per symbol ($T_s = T$), over flat fading channels is a special case of our generalized MAP equalizer. The derivation of the demodulator in [14] and [19] relies on the fact that $\tilde{\mathbf{X}}\tilde{\mathbf{X}}^H = \mathbf{I}$ to arrive at the following expression [19, eq. (14)]:

$$\tilde{x}_k^* \hat{z}_{k,ij} = \sum_{m=1}^p c_m \tilde{x}_{k-m}^* z_{k-m} \quad (17)$$

which can easily be shown to be a rewriting of (16) multiplied by \tilde{x}_k^* . We also note that the demodulators of [14] and [19] were obtained using *remodulation* arguments. We have therefore shown that remodulation is consistent with the MMSE approach.

V. SIMULATIONS

In this section, the performance of our new generalized MAP equalizer is demonstrated via Monte Carlo simulation.

A. Pilot Symbols

When using PSK modulation schemes, a phase ambiguity is inherent at the receiver, caused by unknown phase offset in the channel. Pilot symbols may be used to resolve this ambiguity. The question then arises as to how often a pilot symbol should be sent. The insertion of pilot symbols incurs a signal-to-noise ratio (SNR) penalty of $10 \log_{10}((d+p)/d)$ dB, where $p : d$ is the ratio of pilot to data symbols transmitted.

An important result is that, for the expanded MAP equalizer, the appropriate rate for inserting pilot symbols is dominated by the need to resolve the phase ambiguity, and not the need to effectively sample the fading channel response. In conventional pilot symbol-aided modulation-demodulation (PSAM) schemes [25], where a single channel estimate is formed

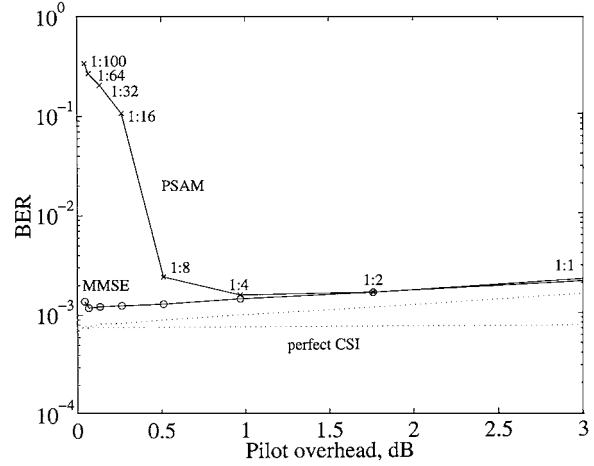


Fig. 3. Effect of pilot symbol rate on BER performance, uncoded system, $E_b/N_o = 25$ dB, $f_{D_{\max}}T = 0.05$ flat fading channel, MMSE prediction $m = 6$, PSAM prediction $K = 11$, and block length 4096. The BER for perfect CSI excluding and including pilot overhead is shown for reference.

by interpolating between estimates obtained from the pilot symbols, the Nyquist sampling criterion must be satisfied; the channel function is effectively being sampled. For example, for a fading rate of $f_{D_{\max}}T = 0.05$, the ratio 1:9 corresponds to the Nyquist rate. In contrast, for an expanded MAP equalizer (or MLSE equalizer employing per-survivor processing, for that matter), there are several channel estimates (one for each state). When the pilot symbol occurs, only those transitions and states consistent with the pilot symbol have a nonzero probability. The phase ambiguity is resolved at that symbol time, since the competing hypotheses and channel estimates with the incorrect phase are eliminated. The phase certainty during neighboring symbol times deteriorates due to uncertainty being introduced by unknown data. At high SNR, the incorrect hypotheses have less effect, and therefore phase certainty lasts longer.

The fundamental difference between our expanded trellis MMSE approach and PSAM (with a MAP receiver) can be seen in Fig. 3. In this example, the bit error rate (BER) has been plotted against the pilot symbol overhead in SNR. The channel is flat fading with $f_{D_{\max}}T = 0.05$, and E_b/N_o was fixed to 25 dB. The block length was chosen to be 4096. For the expanded trellis MMSE, the predictor order was chosen to be $m = 6$ and, for PSAM, the predictor order was $K = 11$ (as in [25]). For reference, the BER for perfect channel state information (CSI) is also shown, both with and without the pilot overhead. This was achieved using the MAP algorithm with perfect CSI and no trellis expansion.

Obviously, there is an optimum choice of pilot symbol rate for a given scenario. Even without the pilot symbol penalty in SNR, the BER rate will never achieve the lower bound associated with perfect CSI since there is a residual loss due to the finite prediction error for both expanded trellis MMSE and PSAM.

For our expanded trellis with MMSE, the need for so many pilot symbols subsides for higher E_b/N_o . This can be explained by the fact that the algorithm performs joint channel and data estimation and at high SNR the incorrect hypotheses have less effect and phase certainty lasts longer. This behavior is seen in Fig. 4. As expected, this behavior is not observed for the

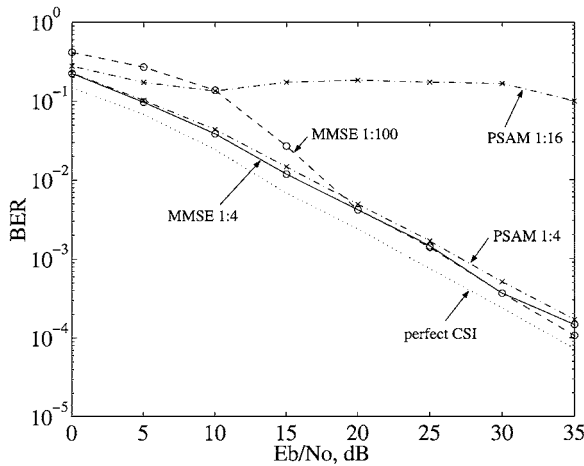


Fig. 4. BER versus E_b/N_o performance for different pilot rates, uncoded system, $f_{D_{max}}T = 0.05$ flat fading channel, MMSE prediction $m = 6$, PSAM prediction $K = 11$, and block length 4096. The BER for perfect CSI excluding pilot overhead is shown for reference.

PSAM receiver, whose performance is dependent on satisfying the Nyquist sampling criterion.

Pilot symbols are not required when there is no phase ambiguity to be resolved. Thus, the generalized MAP equalizer may be operated without pilot symbols for such modulation schemes. Often phase ambiguity is overcome using differential encoding, and, in fact, a version of the generalized MAP algorithm for DPSK systems is possible (see [26] for the flat fading case). This algorithm requires only the reference symbol (a form of pilot symbol) at the beginning of each block. Since resolving the phase ambiguity is not an issue, there is no benefit in inserting further pilot symbols.

B. Prediction Order

The order of the MMSE predictor (or filter) in our new generalized MAP equalizer affects both the performance of the algorithm and the size of the state space (i.e., computational complexity). For a given scenario, the appropriate order of the predictor may be determined from the inspection of the average prediction error. When the reduction in prediction error is not significant for the increase in complexity, the appropriate prediction order has been reached.

This type of analysis as a function of fading rate is relatively straightforward in the flat fading scenario with PSK modulation, but becomes complicated for frequency-selective channels and other modulation schemes. Since it is not possible to perform this kind of analysis for every possible scenario, some general observations are useful. For faster fading systems, a shorter prediction order is suitable, since the coherence time of the channel is shorter. With increasing ISI in the equivalent channel, a longer predictor is required to adequately resolve the ISI. This will be demonstrated in Section V-C.

Fig. 5 shows the improvement in BER performance as a function of increased predictor order for a MAP receiver, using either PSAM channel estimation or our expanded trellis MMSE estimation. Again the channel is flat fading with $f_{D_{max}}T = 0.05$, and E_b/N_o was fixed to 25 dB. PSK modulation was used with a pilot symbol rate of 1:8 and a block length of 4096. Also shown

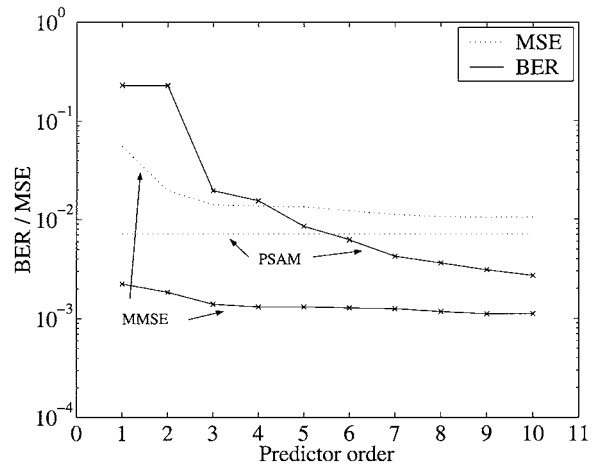


Fig. 5. Effect of predictor order on MSE and BER performance for both PSAM and MMSE channel estimation, BPSK on a flat-fading channel with $f_{D_{max}}T = 0.05$, $E_b/N_o = 25$ dB, pilot symbols 1:8, and block length 4096.

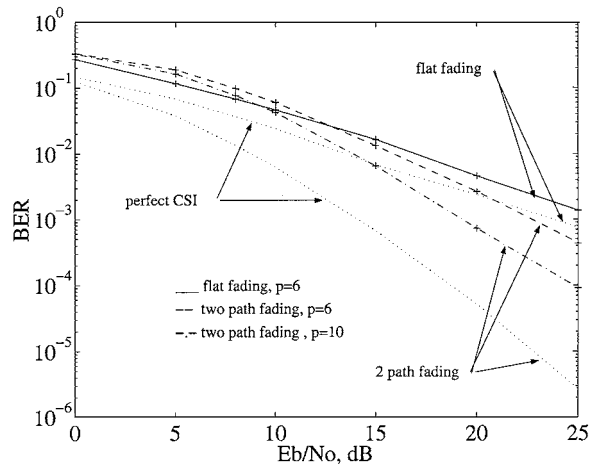


Fig. 6. BER performance of the expanded trellis equalizer for uncoded BPSK system, $f_{D_{max}}T = 0.05$, frequency-flat and frequency-selective equivalent channels. Perfect CSI curves (without pilot symbols) are also shown.

is the corresponding average prediction error. Although less pronounced at 25 dB than at low SNR, the direct relationship between the MMSE prediction error and the BER performance of the new equalizer can be seen. This is in contrast with the PSAM channel estimation.

C. SNR Performance

The performance of the expanded trellis MAP equalizer in frequency-flat and frequency-selective fading channels was characterized in terms of BER as a function of the SNR per bit, E_b/N_o . The example in Fig. 6 is for a binary PSK system with normalized fading rate $f_{D_{max}}T = 0.05$. Pilot symbols were injected in the ratio 1:8.

For the frequency-flat scenario, the sampling rate was chosen to be the same as the symbol rate to allow comparison with well-known results for receivers with perfect CSI, e.g., [1]. The prediction order was chosen to be $P = p = 6$.

For the frequency-selective scenario, a physical channel with two equal power paths spaced at the symbol period T was simulated, and the pulse shape was chosen to be a root-raised cosine pulse with 100% excess bandwidth. In this case, the sam-

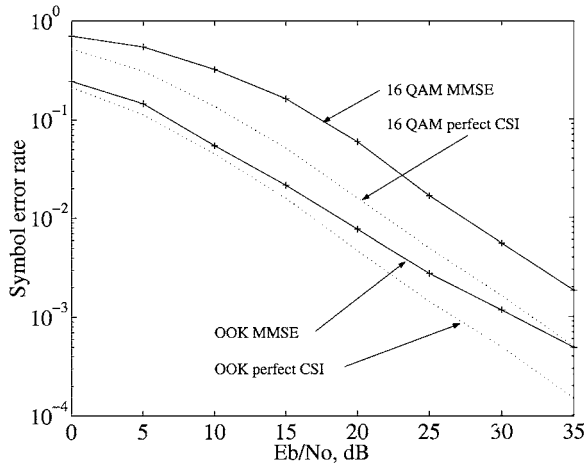


Fig. 7. BER performance of the expanded trellis equalizer for uncoded OOK and QAM systems, $f_{D_{\max}}T = 0.05$, frequency-flat channel. Pilot symbols 1:8 were used to resolve the phase ambiguity for QAM. Perfect CSI curves (without pilot symbols) are also shown.

pling period was chosen to be $T/2$, i.e., $R = 1/2$, satisfying the Nyquist sampling rate and ensuring that the BER performance is unaffected by the sampling phase at the receiver. Fig. 6 shows the results for predictor orders $p = 6$ and $p = 10$.

For reference, Fig. 6 also shows the BER curves for a receiver utilizing perfect CSI (with no pilot symbols).

Although the performance of the receiver is expected to be better with increased diversity, Fig. 6 shows that this is only that case when the predictor order is sufficient for providing good channel estimates. In particular, note that there is a cross-over point with the flat-fading scenario.

To highlight the versatility of the new receiver, the BER performance was also characterized for on-off keying (OOK) ($Q = 2$), and quadrature amplitude modulation (QAM) with $Q = 16$. The flat-fading channel with $f_{D_{\max}}T = 0.05$ was used, with pilot symbols injected at 1:8 to resolve the phase ambiguity for the QAM case. For OOK, $P = p = 6$ was used, and for QAM $P = p = 2$. The result is shown in Fig. 7 where the perfect CSI curves are shown for reference.

Other parameters of interest include the fading rate and the amount of excess bandwidth. These studies are not shown here but the reader is referred to [25] which shows results for a PSAM receiver. For our new receiver, the trends will be the same as the underlying mechanisms are unchanged. For slower fading rates, the BER improves. For higher excess bandwidth, the effective length of the pulse shape is shorter and hence the discrete equivalent channel exhibits less ISI. Thus, with decreasing excess bandwidth, ISI is increased and once again the tradeoff of diversity with channel estimation becomes an issue.

Our receiver has been designed for a system with a single antenna. It is easily modified for diversity reception in a similar manner to receivers proposed in [21], [20], and [23]. Diversity reception is expected to improve BER performance.

D. Turbo Receiver Simulations

As stated in Section I, a soft-output APP equalizer allows for a turbo receiver structure (Fig. 2). The simulated BER performance of a BPSK coded system is shown in Figs. 8 and 9. In both

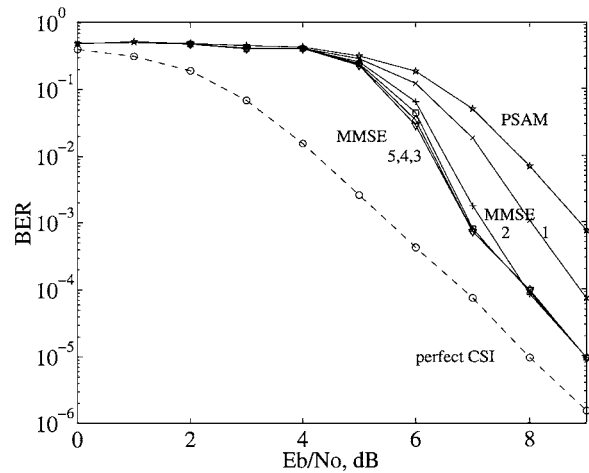


Fig. 8. BER performance for a coded BPSK system using expanded trellis equalizer in turbo system, compared with APP demodulator with PSAM, flat fading channel, $f_{D_{\max}}T = 0.05$, pilots 1:8, $P = p = 6$ for MMSE prediction, $K = 11$ for PSAM. For reference, perfect CSI performance (not including pilot symbols) is shown.

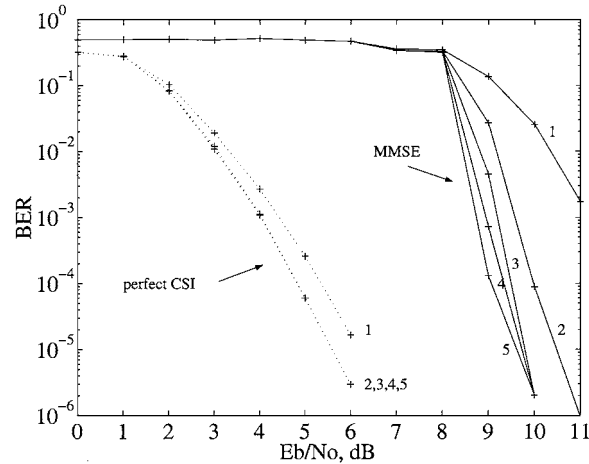


Fig. 9. BER performance for a coded BPSK system using an APP equalizer in turbo system, T -spaced equal power two path fading channels, $f_{D_{\max}}T = 0.05$, pilots 1:8, $p = 6$ for MMSE prediction. For comparison, perfect CSI performance (not including pilot symbols) is shown.

cases, the system uses rate $1/2$ convolutional encoding with 64 states [generators (133 171)] and a block interleaver (128×32 corresponding to an equalization block length of 4096). The pilot rate was 1:8.

In Fig. 8, the channel was flat with normalized fading rate $f_{D_{\max}}T = 0.05$. Results are shown for a receiver with perfect CSI, a receiver using an APP equalizer (demodulator) with PSAM ($K = 11$), and a receiver using our expanded trellis equalizer ($P = p = 6$). The perfect CSI curve is shown for reference. The first iteration corresponds to a coded system with just one equalization and decoding cycle. Note that for perfect CSI and PSAM equalization, there is no benefit from the turbo iterations since the channel has no memory. For the expanded trellis equalizer, benefit is gained with the turbo iterations since the equalizer inherently introduces memory into the trellis according to the predictor model.

Fig. 9 shows results for an ISI channel with T -spaced paths (as in Section V-C). PSAM is not suitable for such a delay

spread environment. For a receiver using perfect CSI, very little benefit is derived past the second turbo iteration. In contrast when the channel is being predicted using the expanded trellis ($p = 6$), a greater number of iterations are need to achieve low BER. In general, the appropriate number of iterations depends on both E_b/N_o and the channel estimator performance. Reflecting the uncoded results, at lower SNR, this system is unable to adequately estimate the channel in the noise, and the BER is poor.

VI. CONCLUSION

In this paper, we have presented a new generalized MAP approach to joint equalization and estimation of frequency-selective and frequency-flat fast-fading channels. Importantly, the algorithm is applicable to modulation schemes with arbitrary envelope. Many previous contributions in MAP (and MLSE) equalization can be seen as specific cases of our new general approach. Simulations demonstrate the good performance of the proposed equalizer.

APPENDIX

Since the original submission of this paper we note that a number of related papers have appeared in the literature [27]–[29].

REFERENCES

- [1] J. Proakis, *Digital Communications*, 3rd ed. New York: McGraw-Hill, 1995.
- [2] H. Meyr, M. Moeneclaey, and S. A. Fechtel, *Digital Communication Receivers: Synchronization, Channel Estimation and Signal Processing*. New York: Wiley, 1997.
- [3] L. M. Davis, I. B. Collings, and R. J. Evans, "Extended least squares identification of doubly spread mobile communication channels," in *Proc. Int. Conf. on Telecommunications (ICT'97)*, vol. 3, Melbourne, Victoria, Australia, Apr. 1997, pp. 1023–1028.
- [4] R. Raheli, A. Polydoros, and C.-K. Tzou, "Per-survivor processing: A general approach to MLSE in uncertain environments," *IEEE Trans. Commun.*, vol. 43, pp. 354–364, Feb. 1995.
- [5] C. Berrou, A. Glavieux, and P. Thitimajshima, "Near Shannon limit error-correcting coding and decoding: Turbo-codes," *Proc. IEEE Int. Conf. on Communications (ICC'93)*, pp. 1064–1070, May 1993.
- [6] P. Hoeher, "Advances in soft-output decoding," *Proc. IEEE Globecom'93*, pp. 793–797, Nov. 1993.
- [7] Y. Li, B. Vucetic, and Y. Sato, "Optimal soft-output detection for channels with intersymbol interference," *IEEE Trans. Inform. Theory*, vol. 41, pp. 704–713, May 1995.
- [8] R. W. Chang and J. C. Hancock, "On receiver structures for channels having memory," *IEEE Trans. Inform. Theory*, vol. 12, pp. 463–468, Oct. 1966.
- [9] L. R. Rabiner, "A tutorial on hidden Markov models and selected applications in speech recognition," *Proc. IEEE*, vol. 77, pp. 257–285, Feb. 1989.
- [10] K. Abend and B. D. Fritchman, "Statistical detection for communication channels with intersymbol interference," *Proc. IEEE*, vol. 58, pp. 779–785, May 1970.
- [11] L. R. Bahl, J. Cocke, F. Jelinek, and J. Raviv, "Optimal decoding of linear codes for minimizing symbol error rate," *IEEE Trans. Inform. Theory*, vol. IT-20, pp. 284–287, Mar. 1974.
- [12] W. Koch and A. Baier, "Optimum and sub-optimum detection of coded data disturbed by time-varying intersymbol interference," *Proc. IEEE Globecom'90*, pp. 807.5.1–807.5.6, Dec. 1990.

- [13] J. A. Erfanian, S. Pasupathy, and P. G. Gulak, "Reduced complexity symbol detectors with parallel structures for ISI channels," *IEEE Trans. Commun.*, vol. 42, pp. 1661–1671, Feb./Mar./Apr. 1994.
- [14] M. J. Gertsman and J. H. Lodge, "Symbol-by-symbol MAP demodulation of CPM and PSK signals on Rayleigh flat-fading channels," *IEEE Trans. Commun.*, vol. 45, pp. 788–799, July 1997.
- [15] R. A. Altis, J. J. Shynk, and K. Giridhar, "Bayesian algorithms for blind equalization using parallel adaptive filters," *IEEE Trans. Commun.*, vol. 42, pp. 1017–1032, Mar. 1994.
- [16] J. P. Seymour and M. P. Fitz, "Near-optimal symbol-by-symbol detection schemes for flat rayleigh fading," *IEEE Trans. Commun.*, vol. 43, pp. 1525–1533, Feb./Mar./Apr. 1995.
- [17] G. Lee, S. B. Gelfand, and M. P. Fitz, "Bayesian techniques for blind deconvolution," *IEEE Trans. Commun.*, vol. 44, pp. 826–835, July 1996.
- [18] Y. Zhang, M. P. Fitz, and S. B. Gelfand, "Soft output demodulation on frequency-selective rayleigh fading channels using AR models," *Proc. IEEE Globecom'97*, pp. 327–330, Nov. 1997.
- [19] J. H. Lodge and M. L. Moher, "Maximum likelihood sequence estimation of CPM signals transmitted over Rayleigh flat-fading channels," *IEEE Trans. Commun.*, vol. 38, pp. 787–794, June 1990.
- [20] X. Yu and S. Pasupathy, "Innovations-based MLSE for Rayleigh fading channels," *IEEE Trans. Commun.*, vol. 43, pp. 1534–1544, Feb./Mar./Apr. 1995.
- [21] Q. Dai and E. Shwedyk, "Detection of bandlimited signals over frequency selective Rayleigh fading channels," *IEEE Trans. Commun.*, vol. 42, pp. 941–950, Apr. 1994.
- [22] P. Hoeher, "A statistical discrete-time model for the WSSUS multipath channel," *IEEE Trans. Veh. Technol.*, vol. 41, pp. 461–468, Nov. 1992.
- [23] M. E. Rollins and S. J. Simmons, "Simplified per-survivor kalman processing in fast-fading frequency selective channels," *IEEE Trans. Commun.*, vol. 45, pp. 544–553, May 1997.
- [24] I. B. Collings and J. B. Moore, "An adaptive hidden Markov model approach to FM and M -ary DPSK demodulation in noisy fading channels," *Signal Processing*, vol. 47, pp. 71–84, Nov. 1995.
- [25] J. K. Cavers, "An analysis of pilot symbol assisted modulation for Rayleigh fading channels," *IEEE Trans. Veh. Technol.*, vol. 40, pp. 686–693, Nov. 1991.
- [26] P. Hoeher and J. Lodge, "Iterative decoding/demodulation for coded DPSK systems," *Proc. IEEE Globecom'98*, vol. 1, pp. 598–603, Nov. 1998.
- [27] E. Baccarelli and R. Cusani, "Combined channel estimation and data detection using soft statistics for frequency-selective fast-fading digital links," *IEEE Trans. Commun.*, vol. 46, pp. 424–427, Apr. 1998.
- [28] A. Anastasopoulos and K. M. Chugg, "Adaptive soft-input soft-output algorithms for iterative detection with parametric uncertainty," *IEEE Trans. Commun.*, vol. 48, pp. 1638–1649, Oct. 2000.
- [29] B. D. Hart and S. Pasupathy, "Innovations-based MAP detection for time-varying frequency selective channels," *IEEE Trans. Commun.*, vol. 48, pp. 1507–1519, Sept. 2000.



Linda M. Davis (S'92–M'94) received the B.E. (Elec.) degree from the University of Adelaide in 1994 and the Ph.D. degree from the University of Melbourne in 1999.

She is a Wireless Research Engineer with Bell Laboratories, Lucent Technologies, Sydney, Australia, having joined the team in March 2000. She researches and develops novel algorithms and architectures for mobile communication, receivers, and her particular research interests include channel identification, estimation, equalization, and decoding. Previously, she held research and lecturing positions at the Australian Defence Science and Technology Organization (1993–1995) and the University of Adelaide (1999), respectively. In addition to her research role, she is active in promoting science, engineering and technology research, innovation and entrepreneurship to engineers and the wider community.



Iain B. Collings (S'92–M'95) was born in Melbourne, Australia, in 1970. He received the B.E. degree in electrical and electronic engineering from the University of Melbourne in 1992 and the Ph.D. degree in systems engineering from the Australian National University in 1995.

In 1995, he was a Research Fellow in the Australian Cooperative Research Center for Sensor Signal and Information Processing, where he worked in the area of radar signal processing. From 1996 to 1999, he was a Lecturer at the University of Melbourne, and since 1999 he has been a Senior Lecturer in the School of Electrical and Information Engineering, at the University of Sydney, Australia. His current research interests include synchronization, channel estimation, equalization, and multi-carrier modulation, for time-varying and frequency-selective channels.



Peter Hoher (M'90–SM'97) was born in Cologne, Germany, in 1962. He received the Dipl.-Eng. and Dr.-Eng. degrees in electrical engineering from the Technical University of Aachen, Germany, and the University of Kaiserslautern, Germany, in 1986 and 1990, respectively.

From October 1986 to September 1998, he was with the German Aerospace Center (DLR), Oberpfaffenhofen, Germany. From December 1991 to November 1992, he was on leave at AT&T Bell Laboratories, Murray Hill, NJ. In October 1998, he joined the University of Kiel, Kiel, Germany, where he is currently a Professor in Electrical Engineering. His research interests are in the general area of communications theory, including digital modulation techniques, soft-output decoding, equalization and channel estimation, with applications in mobile radio.

Dr. Hoher received the Hugo-Denkmeier-Award'90. He is currently serving as an Associate Editor for the IEEE TRANSACTIONS ON COMMUNICATIONS.